CORE
Metadata, citation and similar papers at core.ac
Provided by Elsevier - Publisher Connector

Ion Source Emittance Influence on the Transmission of a Quadrupole Operated in the Second Stability Region

D. J. Douglas
Department of Chemistry, University of British Columbia, Vancouver, B. C., Canada

N. V. Konenkov
Department of General Physics, Ryazan State Pedagogical University, Ryazan, Russia

The variation of transmission (T) with resolution (R) has been calculated for a quadrupole mass filter operated in the second stability region with Mathieu parameters $q = 7.547$ and $a = 0$ to 0.02995. The fringing fields at the entrance to the quadrupole, which can be strongly defocusing, and which can dramatically reduce the acceptance, have been included in the calculation. Even in the absence of fringing fields, at a resolution of 10,000 the acceptance in the x and y directions is less than $2 \times 10^{-4}\ \pi r_0^4 f^2$, which is about 10^{-3} of the acceptance in the first stability region at low resolution. Because the source emittance can strongly effect the $T(R)$ behavior, the calculation of ion transmission has been done for two source emittances that correspond to different degrees of focusing of ions into the quadrupole. The $T(R)$ characteristics for two realistic source emittances give behavior markedly different from the decrease in acceptance with increasing resolution which previously has been used as a measure of the quadrupole transmission. Comparisons of the calculated transmission losses with increasing resolution to earlier experimental results obtained with an inductively coupled plasma source show good agreement provided an emittance which corresponds to ions being tightly focused into the quadrupole is used. The calculation demonstrates that up to a resolution at half height of 7000 in the experiment, the transmission losses were a result of the decreasing quadrupole acceptance. At higher resolution the experimental transmission was limited by either the residence time of the ions in the quadrupole or the rod quality. It is also shown that the strong defocusing effects of the fringing fields at the entrance of the quadrupole can be largely overcome by accelerating the ions through these fields and then decelerating the ions in the quadrupole. (J Am Soc Mass Spectrom 1998, 9, 1074–1080) © 1998 American Society for Mass Spectrometry

For any real scanning mass analyzer the transmission decreases as the resolution is increased [1]. The performance of a mass spectrometer is strongly tied to this variation of transmission (T) with resolution (R). For a sector mass analyzer, narrow entrance and exit slits reduce the transmission at high resolution. For a quadrupole mass analyzer there are no physical apertures or slits required to control the resolution. However, there is an "electronic" aperture, the acceptance, which decreases as resolution increases [2]. The acceptance is the area of a region in phase space with combinations of transverse position and velocity that are transmitted by the mass filter. Because the ion motion in the x and y directions of a quadrupole mass analyzer are independent, the acceptance can be defined separately for each direction. The acceptance decreases as the resolution increases; this normally decreases the sensitivity [2]. The extent to which the sensitivity decreases with increasing resolution is dependent upon the distribution in phase space of ions from the source, i.e., the source emittance.

Ion motion in quadrupole mass filters is described in terms of the Mathieu parameters a and q defined by

$$a = \frac{8eU}{m\omega^2 r_0^2} \tag{1}$$

and

$$q = \frac{4eV}{m\omega^2 r_0^2} \tag{2}$$

where e is the ion charge, U is the dc voltage applied from each quadrupole rod to ground, V is the 0 to peak radio frequency (rf) voltage applied between each rod

Address reprint requests to Dr. N. V. Konenkov, Department of General Physics, Ryazan Pedagogical University, Svoboda Str. 46, 390000, Ryazan, Russia. E-mail: konenkov@ttc.ryagan.ru

© 1998 American Society for Mass Spectrometry. Published by Elsevier Science Inc.
1044-0305/98/$19.00
PII S1044-0305(98)00077-4

Received December 12, 1997
Revised May 12, 1998
Accepted May 12, 1998

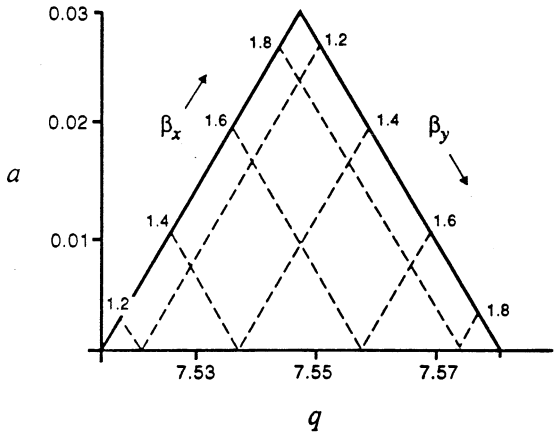

Figure 1. The second stability region. The Mathieu parameters a and q are defined by eqs 1 and 2. The fundamental frequency of ion motion, Ω, is determined by β values: $\Omega = (\beta - 1)\omega/2$ $(1 < \beta \leq 1.5)$ and $\Omega = (2 - \beta)\omega/2$ $(1.5 < \beta < 2)$ [3].

and ground, m is the ion mass, ω is the angular radio frequency applied to the rods, and r_0 is the field radius of the quadrupole (the distance from the center to a rod). Combinations of a and q giving ion motion simultaneously stable in the x and y directions are usually shown on a stability diagram. The "second" stability region (notation from [2]) is shown in Figure 1. This region allows a resolution of several thousand at $m/z \approx 100$ with a conventional quadrupole rod set [3]. To obtain this resolution with operation in the first stability region requires an exceptionally long (3 m or more) rod set [4]. The high resolution is of practical interest for inductively coupled plasma mass spectrometry (ICP-MS) or other forms of elemental mass spectrometry, where it can be applied to separate atomic ions from molecular ions of the same nominal mass [5]. To obtain high resolution the ion energy must be relatively low, on the order of tens of eV. However operation in the second stability region can also be used to give *unit* resolution on ions with energies up to several keV [6, 7]. These attractive features are offset by the lower sensitivity of the quadrupole caused by the strongly defocusing fringing fields at the entrance of the quadrupole and by the relatively small quadrupole acceptance at high resolution.

The variation of transmission with resolution of a quadrupole mass filter can depend on many factors such as the frequency and field radius (which scale the acceptance [2]), fringing fields [3, 8], the quadrupole field quality [2, 9, 10], the emittance of the ion source [11], the ion residence time in the quadrupole field [2, 3, 12, 13], and the alignment of the ion source with the quadrupole. The acceptance of a quadrupole operated in the second stability region has been calculated by Dawson and Binqi [3] and also by Titov [10]. In both cases the fringing fields at the quadrupole entrance were included in the calculation and were shown to dramatically reduce the quadrupole acceptance. Titov also showed that field imperfections can decrease the quadrupole acceptance. In this previous work it was recognized that the source emittance could change the transmission resolution characteristics, but the effect of the source emittance was not included in the calculations. The combined acceptance in the x and y directions was simply taken as a measure of the relative quadrupole sensitivities at different resolutions.

In this work we have calculated the transmission resolution characteristics $[T(R)]$ of a quadrupole operated in the second stability region for two different source emittances which differ in the extent to which ions are focused into the quadrupole. The calculation also includes the fringing fields at the quadrupole entrance. We assume the residence time in the quadrupole is sufficiently high that it does not limit the resolution and assume an ideal quadrupole field. Even in the absence of fringing fields, at a resolution of 10,000 the acceptance is less than 2×10^{-4} $\pi r_0^4 f^2$, which is about 10^{-3} of the acceptance in the first stability region at low resolution. It is shown that when a realistic source emittance is included in the calculation, the variation of transmission with resolution is markedly different from the variation of acceptance with resolution. Previous experimental measurements [5] of the $T(R)$ behavior obtained with an inductively coupled plasma (ICP) source show a decrease of transmission with increasing resolution which is considerably less than expected from the decrease of acceptance at increasing resolution. The $T(R)$ characteristics of the experiment have been modeled and good agreement with the experiment can only be obtained provided an emittance which corresponds to the ions being tightly focused into the quadrupole is used. The calculation shows that up to a resolution at half height of 7000 the experimental transmission losses were a result of the decreasing quadrupole acceptance; at higher resolution the transmission was limited by the residence time in the quadrupole or by field imperfections. It is also shown that the strong defocusing effects of the fringing fields at the entrance of the quadrupole can be largely overcome by accelerating the ions through these fields and then decelerating the ions in the quadrupole.

Methods

The transmission T of a quadrupole is the ratio

$$T = I_{\text{out}}/I_{\text{in}} \tag{3}$$

where I_{out} is the output current and I_{in} is the input current. It may be calculated by dividing the input aperture into a number of points and considering the transmission at each point. Formally this can be written

$$T = \left(\sum_{i=1}^{P} \sum_{k=1}^{K} \sum_{j=1}^{J} T_{ik}^{x} T_{ij}^{y} \right) \Big/ PKJ \tag{4}$$

where $e*P*K*J*f = I_{in}$ is the input ion current, e is the ion charge, f is the rf frequency, P is the number of initial phases ξ_i over one rf cycle [$\xi = (\omega t)/2$], k and j refer to initial points x_k, y_j on the input aperture in the x and y directions, and K and J are the number of points in the x and y directions, respectively. T^x_{ik} and T^y_{ij} are elements of the transmission matrix for the x and y transverse coordinates:

$$T^x_{ik} = 0, \quad \text{if } x_{max} > r_0, \quad T^x_{ik} = 1, \quad \text{if } x_{max} < r_0$$

and

$$T^y_{ij} = 0, \quad \text{if } y_{max} > r_0, \quad T^y_{ij} = 1, \quad \text{if } y_{max} > r_0 \qquad (5)$$

where x_{max} and y_{max} are the maximum oscillation amplitudes of a trajectory in the x and y directions, respectively. The product $T^x_{ik}T^y_{ij}$ indicates that the ions must be transmitted at the same rf input phase ξ_i in both the x and y directions simultaneously. In general, the distribution of ion current on the input aperture is determined by the ion source emittance. Here, to calculate the acceptance, we assume a uniform distribution of ions on the input aperture. For a quadrupole field, the maximum oscillation amplitudes u_{max} (x_{max} and y_{max}) may be calculated from [2]

$$u_{maxl} = \sqrt{B_{max}}\ \sqrt{\Gamma(\xi_i)u_l^2 + 2A(\xi_i)u_l\dot{u}_l + B(\xi_i)\dot{u}_l^2} \qquad (6)$$

where l refers to either x or y, A, B, and Γ are acceptance ellipse parameters modified by the fringing field, u and $\dot{u}$ are initial transverse ion position and velocity, B_{max} is the maximum value of B on the interval $0 < \xi < \pi$. For the most general case, for the transmission calculation, it is necessary to know both the ion source emittance and acceptance ellipse parameters A, B, and Γ at given input rf initial phases ξ_i.

As in [14] we use the approach developed by Dawson [11] for calculating the modified parameters A, B, and Γ, taking into account the input fringing field. Here we use the fringing field model of McIntosh and Hunter [15] where the ion motion in the fringing field is described by

$$\frac{d^2x}{d\xi^2} + [a + 2q\cos 2(\xi - \xi_0)]xf(z) = 0 \qquad (7)$$

$$\frac{d^2y}{d\xi^2} + [a + 2q\cos 2(\xi - \xi_0)]yf(z) = 0 \qquad (8)$$

$$z = 1.5\xi/(\pi n_f) \qquad (9)$$

$$f(z) = 1 - e^{(-2.13z - 1.55z^2)} \qquad (10)$$

The values of x, y, and z are expressed in units of r_0. The coefficients of z in eq 10 are taken from [15] and correspond to the case where the entrance aperture plate is spaced $0.25r_0$ from the end of the quadrupole rods. The numerical calculations show that in this case the quadrupole field increases from zero at the aperture plate to 0.9987 of the full value within the quadrupole over a distance $1.5r_0$ (eq 10 with $z = 1.5$). The numerical calculations also show that penetration of the quadrupole field through the aperture is negligible provided the aperture diameter is $0.5r_0$ or less. In eq 9 n_f is the number of rf cycles that the ions spend in the fringing field with distance $z = 1.5r_0$. In this model of the fringing field the x, y, and z motions remain independent and the fringing field does not change the ion energy.

To find the modified ellipse parameters A, B, and Γ, eqs 7–10 were solved with the initial conditions $u = 0$, $\dot{u} = 1$, and $u = 1$, $\dot{u} = 0$ [2] ($\dot{u} = du/d\xi$) to obtain the transformation matrix for motion through the fringing field. For this a combination of numerical methods was used, as described previously [14]. The Runge–Kutta method was used to initiate the Numerov method which was then used for calculating the ion trajectories. In combination with the Numerov method, the Meisner matrix method was employed to calculate transverse ion velocities. This combined numerical method allows us to solve the above equations with sufficiently high accuracy that the determinant of the transformation matrix did not deviate from 1 by more than 1×10^{-3}. The transformation matrix was then used to calculate modified acceptance ellipses.

Acceptance

The acceptance is defined as the region in the phase–space of the ions composed of transverse velocities $\dot{u}$ and positions u where ions will be transmitted through the mass filter mass [2]. These regions for the x and y directions are described analytically by ellipses. The area of the ellipses divided by π is the acceptance. The ellipses change orientation with initial phase but their areas remain constant. The area depends on the working point (a, q) in the stability diagram and thus depends on the resolution. The fringing field can significantly change these ellipses from those of an ideal mass filter.

For a static ion source with a constant input ion current uniformly distributed in phase space Dawson [11] introduced the "average" acceptance. This is characterized by contours in the phase–space plane (u, $\dot{u}$) with a given fraction of transmission. The boundary of the acceptance defined this way may be determined at different transmission levels p. The value p represents the probability that ions which have initial conditions within the contours will be transmitted, averaged over all phases. To calculate this time-averaged transmission requires calculating the ratio N_c/N, where N_c is the number of ellipses that contain the given point on a contour and N is the total number of all initial phase numbers calculated. Here we have used $N = 100$.

Figure 2a, b, c illustrate the change of the quadrupole

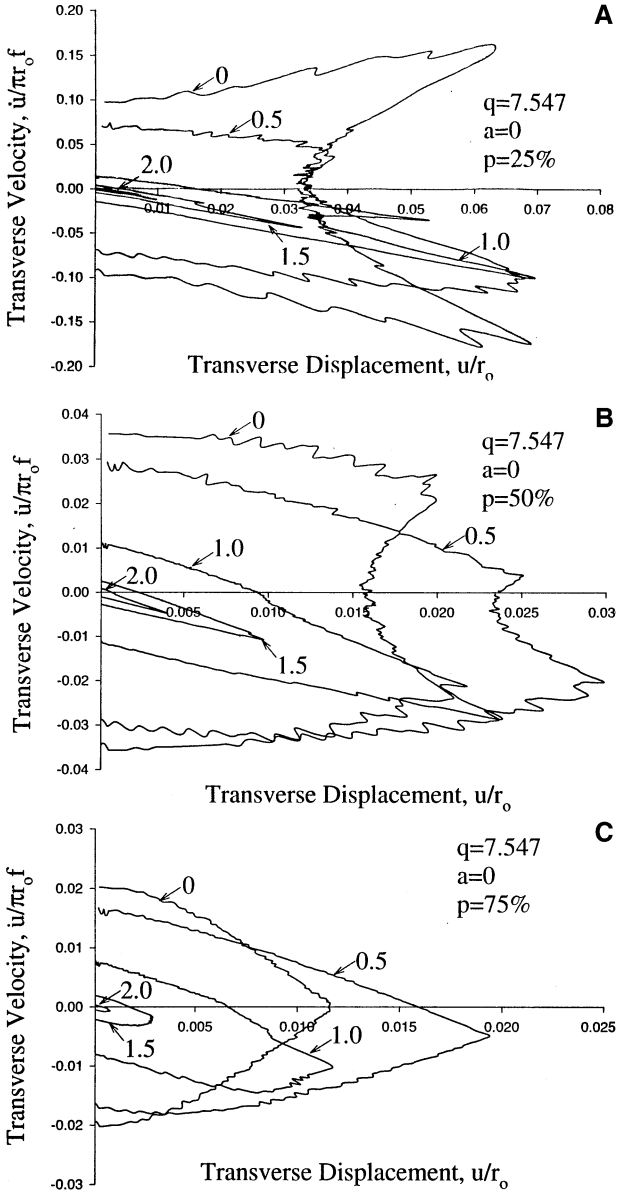

Figure 2. Acceptance contours at the working point $a = 0$, $q = 7.547$ ($R = 114$): (**a**) 25%, (**b**) 50%, and (**c**) 75% transmission level, for values of $n_f = 0$, 0.5, 1.0, 1.5, and 2.0.

acceptance caused by the input fringing field at the working point $a = 0$, $q = 7.547$ ($R = 114$). The 25% contours at different given numbers of cycles that the ions spend in the fringing field, n_f, are given in Figure 2a. Similar data for 50% and 75% transmission levels are shown in Figure 2b, c. The fine structure of the contours is caused by the finite number of ellipses that were used in the calculation and introduces some uncertainty in the position of the contours. Each curve in Figure 2 is marked by the number of rf cycles, n_f, which the ions spend in the fringing field, with $z_f = 1.5r_0$. The value $n_f = 0$ corresponds to the case where the fringing field is absent or the axial ion velocities are large. Figure 2 demonstrates that the acceptance can be very complex for the second stability region.

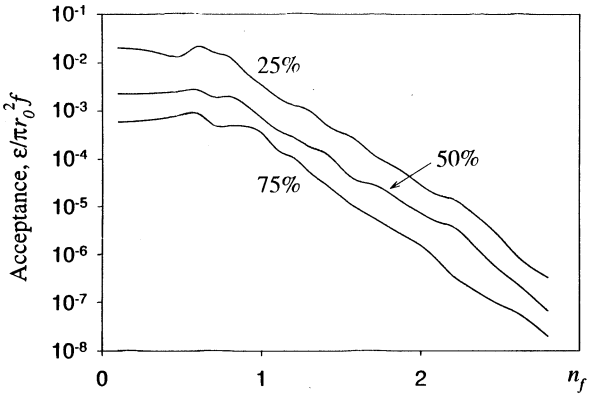

Figure 3. Acceptance of the quadrupole for different numbers of rf cycles in the fringing field, n_f, for $a = 0$, $q = 7.547$.

From Figure 2 it is seen that at low values of n_f, the acceptance ellipses are approximately parallel to the u axis. To match this would require a source giving an approximately parallel input beam. At higher values of n_f, which correspond to decreasing axial energies, the ellipses rotate to an angle of about $\pi/4$ to the axis. To match this acceptance would require a focused ion beam (negative $\dot{u}$ for positive u). Thus for the case where $n_f = 1.5$–2.0 the focusing is optimal when the transverse displacement u and velocity $\dot{u}$ are linearly related by $\dot{u} \approx -\pi f u$ (Figure 2b).

Figure 3 gives the dependence of the area of the acceptance ellipses (Figure 2) on the number of cycles, n_f, that the ions spend in the fringing field for different transmission levels p. This behavior is similar to that calculated in [3a] but extends to higher n_f. The number of cycles is given by $n_f = 1.5r_0 f/v_z$, where v_z is the axial ion velocity. Practically no change of acceptance takes place up to about $n_f \approx 0.7$, i.e., when ions pass through the fringing field in 0.7 rf cycles or less. The required ion energy E_z for a given n_f can be calculated as

$$E_z \geq (m/2)(1.5r_0 f/n_f)^2 = 1.17M(r_0 f/n_f)^2 \qquad (11)$$

where M is the ion mass (amu), r_0 is the radius field (cm), and f is the rf frequency (MHz). From eq 11 we calculate that to achieve high transmission the axial energy must be $E_z \geq 70$ eV for typical mass filter parameters: $f = 1.0$ MHz, $r_0 = 7$ mm, $M = 60$ amu, $n_f \leq 0.7$. This high ion energy decreases the resolution that can be achieved. Decreasing the ion energy to improve resolution leads to losses of ion transmission as described by Dawson and Binqi [3]. The results of Figure 3 suggest that the fringing fields will severely limit the ion transmission unless high ion energies are used. However, we show below that the strong defocusing properties of the fringing fields can be largely overcome by accelerating the ions through the fringing fields to decrease n_f and then decelerating the ions in the quadrupole to lower the energy in order to maintain high resolution.

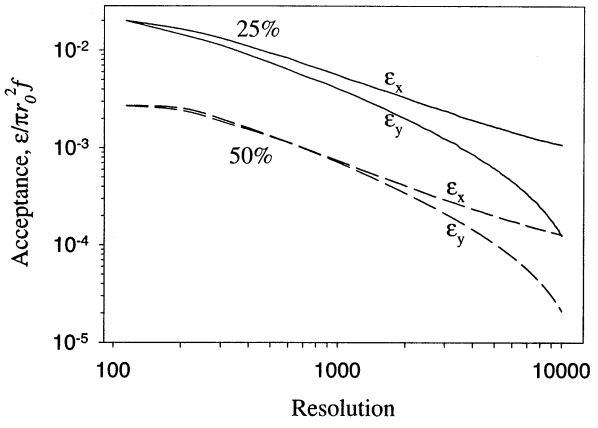

Figure 4. Quadrupole acceptance for the x direction (ε_x) and the y direction (ε_y) vs. resolution R for 25% (solid lines) and 50% (dashed lines) transmission levels.

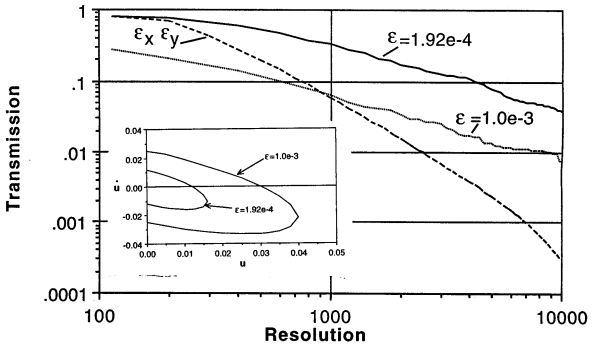

Figure 5. The transmission of the quadrupole vs. resolution for source emittances in both x and y of $1.92 \times 10^{-4}\ \pi r_0 f^2$ (solid line) and $1.0 \times 10^{-3}\ \pi r_0 f^2$ (dotted line). The inset shows the emittance ellipses for these two cases. The combined acceptance (50%) $\varepsilon_x \varepsilon_y$ is shown by the dashed line.

The variation of quadrupole acceptances ε_x and ε_y (the areas of the acceptance ellipses) in the directions x and y for the 25% and 50% transmission level with resolution ($R = q/\Delta q$) are given in Figure 4. Here $n_f = 0.5$. The acceptance ε_y for the y direction decreases more rapidly than that for the x direction. [The x axis passes through the rods with positive dc and the y axis passes through rods with negative dc (for positive ions)]. However, this difference between ε_x and ε_y values is small in comparison with the first and third stability regions [14]. The resolution $R = q/\Delta q$ is related to the working point (a, q) on the stability diagram by

$$a = 0.2955 - 3.3687/R, \qquad q = 7.547 \tag{12}$$

Transmission Versus Resolution

For transmission calculations the integration step size was decreased from $\pi/1000$ to $\pi/4000$. This was necessary to calculate trajectories for high resolutions up to 10,000. A uniform spatial distribution of ions within the source emittance was assumed.

For the idealized case we use two ion source models which correspond to two different quadrupole acceptances. For the first, the 50% contour for $R = 114$, $n_f = 0.5$ was used (Figure 2b). This was approximated by an ellipse described by

$$1.111u^2 + 2 * 0.882u\dot{u} + 1.6\dot{u}^2 = 0.0010 \tag{13}$$

where the source emittance $\varepsilon_x = \varepsilon_y = 0.001\pi r_0^2 f$. The second source model corresponds to the acceptance for $R = 1000$, $p = 50\%$, and $n_f = 0.5$, given approximately by the ellipse

$$1.333u^2 + 2 * 0.882u\dot{u} + 1.333\dot{u}^2 = 1.92 \times 10^{-4} \tag{14}$$

with emittance $1.92 \times 10^{-4}\ \pi r_0^2 f$. These two ellipses are shown in the inset of Figure 5.

Ellipses 13 and 14 determine the initial conditions of the input ion beam. Here it is proposed that ions move with constant velocities $v_z = 3r_0 f$ which gives $n_f = 0.5$, so the fringing fields cause only minor reductions of the acceptance (Figure 3). For an ellipse of the form $\Gamma u^2 + 2Au\dot{u} + B\dot{u}^2 = \varepsilon$ the maximum value of u is given by $u_{\max} = \sqrt{\varepsilon B}$. For the emittance of eq 13 the maximum input beam diameter d is 0.56 mm at typical working conditions: $f = 1.2$ MHz, $r_0 = 7$ mm. For the emittance of eq 14 the maximum diameter is only 0.224 mm. This small diameter requires the use of a strongly focusing lens [16].

The dependence of the calculated transmission T on resolution $R = q/\Delta q$ is shown in Figure 5 for these two emittances. Also shown is the variation of the combined acceptance ($\varepsilon_x \varepsilon_y$, 50%) with R. The combined acceptance has been normalized to the same transmission at $R = 114$ as the source with $\varepsilon = 1.92 \times 10^{-4}$. These data show that a decreased ion source emittance gives a smaller decrease of transmission with increasing resolution because a greater fraction of the ions is within the quadrupole acceptance. The decrease of T with increasing R of the two sources $T(R)$ is similar at $R > 500$. Here the quadrupole acceptance is always less than the source emittance in both cases. As the quadrupole scans over a peak, the acceptance increases from zero to a maximum at the peak center, then decreases to zero. A triangular peak is formed. In the initial part of curves $T(R)$ (at low R) the transmission decreases with resolution more slowly than the combined acceptance, because at $R = 114$ the acceptance coincides with the emittance to some extent (Figure 2). For such an idealized ion source the transmission falls with resolution approximately as $T \approx R^{-1}$ as has been found in detailed modeling of the first stability region [11]. The source with the smaller emittance shows a somewhat smaller decrease in transmission with increasing resolution. For example, as the resolution increases from 114 to 400, the transmission decreases by $\times 0.75$ for $\varepsilon = 1.9 \times 10^{-4}$ and by $\times 0.51$ for $\varepsilon = 1 \times 10^{-3}$.

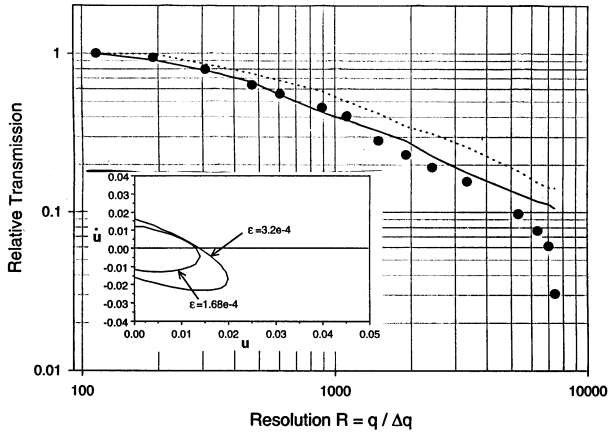

Figure 6. Comparison of calculated transmission to experiment. The points are the experimental data. The solid and dashed lines correspond to source emittances of 3.2×10^{-4} and 1.68×10^{-4}, respectively. The inset shows the emittance ellipses for these two cases.

Comparison to Experiment

The variation of T with R measured in an ICP-MS experiment [5] with $m/z = 59$ (Co^+), 23 eV ion energy, $f = 1.2$ MHz, and $r_0 = 0.7$ cm is shown in Figure 6. In this experiment ions were accelerated to an energy of 163 eV through an aperture plate $0.25\ r_0$ in front of the quadrupole. They were then decelerated to 23 eV in the quadrupole. The calculated transit time through the fringing field (length $1.25\ r_0$) corresponds to $n_f = 0.6$. Empirical tuning of the lenses for the highest sensitivity apparently reached an n_f corresponding to the optimum of Figure 3. Thus acceleration of ions at the entrance of the quadrupole followed by deceleration in the quadrupole can be used to overcome the defocusing effects of the fringing fields. Because the ion energy is low in the quadrupole, high resolution can be maintained. The calculation of the acceptance for Figure 3 used a uniform speed through the fringing field. Repeating the calculation for an ion decelerating through the fringing field but with same total n_f, 0.6, showed that the acceptance was the same. Thus the contours of Figure 2 likely apply reasonably well to the case where the ions are accelerated into the quadrupole through an entrance aperture and then slowed in the mass filter (with the rod offset) as long as the comparison is made at the same n_f.

To compare theory and experiment it is necessary to relate the theoretical resolution $R = q/\Delta q$ to the experimentally determined resolution $R_{1/2}$($R_{1/2} = m/\Delta m_{1/2}$ where m is the mass and $\Delta m_{1/2}$ is the measured peak width at half height). At $a = 0$ (no dc between the pole pairs) $R = 114$ [3, 13, 14]. Experimentally it was found that $R_{1/2} = 167$. From this it follows that $R = q/\Delta q \approx 0.683\ R_{1/2}$. The decrease of transmission with resolution of the experiment over the range $100 < R < 4000$ is considerably less than the decrease of the combined acceptance over the same range. The results of Figure 5 suggest that this can be attributed to source emittance effects.

The ion source emittance of the experiment is not known. An emittance model which gives the same behavior as the experimental curve (Figure 6) is needed. In the initial part of the experimental curve, $T/T(R = 114)$, T decreases only slowly with R. Thus it is reasonable to propose that the source emittance coincides approximately with the 50% acceptance contours at $n_f = 0.6$ in the resolution region $R = 500$–1000. Therefore, we describe the ICP ion source emittance by two ellipses:

$$1.707u^2 + 2.1296u\dot{u} + 1.25\dot{u}^2 = 3.2 \times 10^{-4} \quad (15)$$

$$0.994u^2 + 0.80u\dot{u} + 1.167\dot{u}^2 = 1.68 \times 10^{-4} \quad (16)$$

Equations 15 and 16 correspond to resolutions of 500 and 1000, respectively. These ellipses are shown in the inset of Figure 6.

To compare theory and experiment we normalize the experimental data and calculated transmission to a transmission of 1 at $R = 114$. The calculated $T(R)$ behavior for the two sources is shown in Figure 6 and suggests that the actual ICP emittance lies within about $(2 < \varepsilon < 3) \times 10^{-4}$. The ICP source and ion optics apparently produced a relatively high density input beam focused into the quadrupole. The maximum value of x or y for the ellipse with $\varepsilon = 3.2 \times 10^{-4}$ is $0.04r_0$ or 0.28 mm in this case ($r_0 = 7$ mm). Comparison of the calculated and measured curves suggests that up to $R = 5000$, the decrease in T with R is caused by the decrease in the quadrupole acceptance. At higher resolution the transmission drops sharply, and probably is limited by the transit time through the quadrupole or by the rod quality. This comparison also suggests that the defocusing effects of the fringing field were at least partially overcome by using an entrance aperture at a fairly high accelerating potential. Further gains in ion transmission then will require improved matching of the source to the quadrupole acceptance.

Summary

The results here show that the $T(R)$ characteristics of a quadrupole can depend strongly on the source emittance and can differ markedly from the variation of acceptance with resolution. This has been demonstrated for a quadrupole operated in the second stability region, but these considerations also apply to other stability regions. The $T(R)$ characteristics of an ICP-MS system with a quadrupole operated in the third stability region (a, q) ~ (3, 3) have recently been reported [17] and differ considerably from the variation of acceptance with resolution. The results here suggest that this difference may derive from source emittance effects. The $T(R)$ behavior of a quadrupole can also differ from that of the acceptance of an ideal quadrupole if there are

field imperfections [10]. It would be of interest to calculate $T(R)$ characteristics including the source emittance for this more complex case.

Acknowledgments

This work was supported through an NSERC-SCIEX Industrial Chair. Travel for N. Konenkov to the University of British Columbia was supported by the "Going Global" program of the Canadian Association of University Teachers. The authors thank V. Titov for preprints of [10].

References

1. Brunnee, C. *Int. J. Mass Spectrom. Ion Processes* **1987,** *76,* 125–237.
2. Dawson, P. H. *Quadrupole Mass Spectrometry and Its Applications*; Elsevier; Amsterdam, 1976.
3. (a) Dawson, P. H.; Binqi, Y. *Int. J. Mass Spectrom. Ion Processes* **1984,** *56,* 25–40. (b) *ibid.* **1984,** *56,* 41–50.
4. (a) Paul, W. In *Les Prix Nobel*; Almqvist and Wiskell International; Stockholm, 1989. (b) von Zahn, U. *Z. Phys.* **1962,** *168,* 129–142.
5. Ying, J.-F.; Douglas, D. J. *Rapid Commun. Mass Spectrom.* **1996,** *10,* 649–652.
6. Hiroki, S.; Kanenko, K.; Murakami, Y. *Vacuum* **1995,** *46,* 1445–1447.
7. Grimm, C. C.; Clawson, R.; Short, R. T. *J. Am. Soc. Mass Spectrom.* **1997,** *8,* 539–544.
8. Dawson, P. H. *Adv. Electron. Electron Phys.* **1980,** *53,* 153–208.
9. Von Bush, F.; Paul, W. *Z. Phys.* **1961,** *164,* 588–594.
10. (a) Titov, V. *J. Am. Soc. Mass Spectrom.* **1998,** *9,* 50–69. (b) *ibid.* **1998,** *9,* 70–87.
11. Dawson, P. H. *Int. J. Mass Spectrom. Ion Processes* **1990,** *100,* 41–50.
12. Dawson, P. H. *Int. J. Mass Spectrom. Ion Phys.* **1974,** *14,* 317–337.
13. Konenkov, N. V.; Kratenko, V. I. *Int. J. Mass Spectrom. Ion Processes* **1991,** *108,* 115–136.
14. Konenkov, N. V. *Int. J. Mass Spectrom. Ion Processes* **1993,** *123,* 101–105.
15. McIntosh, B. J.; Hunter, K. L. *Int. J. Mass Spectrom. Ion Processes* **1989,** *87,* 157–164.
16. Shagimuratov, G. I.; Konenkov, N. V.; Mogilchenko, G. A.; Silakov, S. S. *Sov. J. Tech. Phys.* **1990,** *60,* N1, 112–116.
17. Du, Z.; Olney, T. N.; Douglas, D. J. *J. Am. Soc. Mass Spectrom.* **1997,** *8,* 1230–1236.